

Investigations of polymer chains in oriented fluid phases with deuterium nuclear magnetic resonance

Edward T. Samulski

Department of Chemistry and Institute of Materials Science, University of Connecticut
U-136, Storrs, CT 06268, USA

(Received 26 March 1984)

Deuterium nuclear magnetic resonance (D n.m.r.) is a potentially powerful technique for exploring molecular structural and dynamical properties of polymer chains in bulk fluids and concentrated solutions. A variety of systems can be investigated (the solid state, elastomeric networks, sheared polymer fluids, chain solutes in liquid crystal solvents, and polymeric liquid crystals), over a wide range of dimensions (local chain properties, rotational isomeric state parameters, behaviour between network junctions or entanglements, evolution of tube distributions, and domain sizes of homogeneous chain alignment). A coarse comparison of low molar mass liquid crystals with condensed phases of entangled polymer fluids and elastomeric networks illustrates the key features of the D n.m.r. technique and establishes a common framework for interpreting experiments.

(Keywords: deuterium nuclear magnetic resonance; liquid crystal; polymer orientation)

INTRODUCTORY REMARKS

The complex behaviour of both quiescent and non-equilibrium entangled polymer fluids and the associated difficulties of modelling such fluids has challenged experimentalists and theoreticians for much of the history of polymer physics^{1,2}. These challenges are not without significant practical ramifications: extreme, aperiodic flow and shear fields characterize most polymer fabrication processes. This long-standing interest in studies of oriented, fluid polymer phases (melts and solutions) has recently been augmented by the discovery of spontaneously oriented polymer fluids—polymer liquid crystals³. In addition to the intrinsic interests in this peculiar state of matter, polymeric liquid crystals have attracted considerable attention in their own right as such ordered phases are intimately associated with the fabrication of ultra-high strength polymeric materials. Herein we consider the utility of deuterium nuclear magnetic resonance (D n.m.r.) for eliciting structural and dynamical information from oriented, fluid polymer phases. The D.n.m.r. technique continues to prove to be singularly well-suited to the investigation of organization and molecular dynamics in low molar mass liquid crystals⁴. And, since the latter materials may provide a useful paradigm for investigating fluid, macromolecular phases (e.g. polymer solutions or melts under the influence of flow fields, deformed elastomer networks and polymeric liquid crystals), we begin by constructing a coarse, heuristic comparison of low molar mass liquid crystals and entangled flexible polymers. Then the relevant features of the D n.m.r. methodology are reviewed followed by brief summaries of studies employing elastomeric networks subjected to simple tension and compression, sheared polymer fluids, chain solutes dissolved in liquid crystal solvents, and polymeric liquid crystals.

LIQUID CRYSTALS VS. ENTANGLED MACROMOLECULES

A very large number of anisometric, low molar mass organic molecules, molecules exhibiting distinctly different dimensions (prolate or oblate), melt into ordered fluid phases (thermotropic liquid crystals) before forming the conventional isotropic liquid state. There are also examples of low molar mass molecules that form liquid crystalline phases when dissolved (lyotropics). For the most part, however, these latter phases are frequently characterized by specific interactions between the solute and solvent (e.g. an amphiphile in water) resulting in a spontaneously ordered dispersion of anisometric aggregates (rod- or disc-like micelles). Both thermotropic and lyotropic liquid crystals exhibit a remarkable variety of mesophases having supramolecular organization ranging from structures with multiple degrees of translational and orientational order to the simplest, a nematic liquid crystal—an ordered fluid whose constituent molecules have a single degree of orientational order (no translational order). The nematic liquid crystal is a uniaxial phase characterized by anisotropic physical properties, i.e. properties such as the molar refractivity, magnetic (dielectric) susceptibility, etc., which depend on orientation⁵. It is this unique feature of liquid crystals which distinguishes them from ordinary liquids and which is in fact reminiscent of the physical properties of crystals and hence the origin of the nomenclature.

Nematic liquid crystal

For our purposes it will be sufficient to focus on the properties of a thermotropic nematic liquid crystal composed of prolate molecules. In the nematic, each prolate molecule (*mesogen*) maintains its major axis on average parallel to those of its neighbours locally defining a

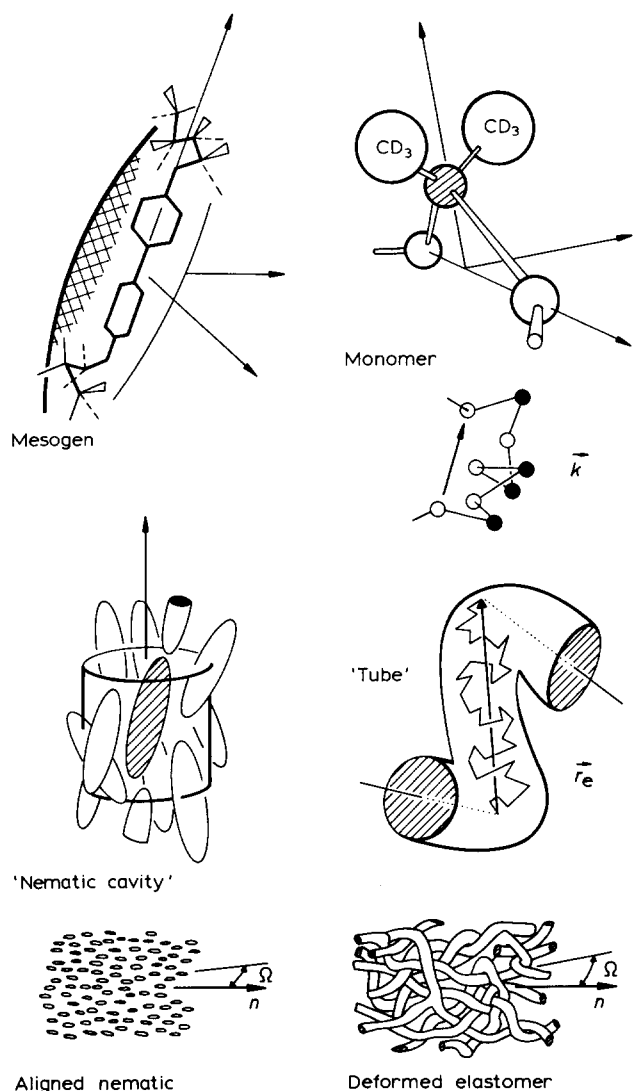


Figure 1 Schematic illustration of the principal structural elements and features of two types of uniaxial, fluid phases: a nematic liquid crystalline melt (left) and an elastomer polymer network (right) subjected to simple tension. The unique direction in each of the fluids, the nematic director and the direction of principal strain, respectively, is denoted \vec{n} . \vec{n} in turn may be oriented at an angle Ω relative to a laboratory coordinate (e.g., the n.m.r. spectrometer magnetic field B)

unique direction in the fluid—the local nematic director \vec{n} . The mesogen librates about \vec{n} under the influence of an anisotropic potential of mean torque. The anisotropic nature of the forces exerted on a mesogen by its neighbours appears to be dominated by repulsive (steric) interactions⁶. This is schematically suggested in Figure 1 by depicting the mesogen in a cylindrical cage. (The nematic cage would transform into a spherical cage on heating to the isotropic melt.) In this representation the axis of the nematic cage would be colinear with the local \vec{n} . In the absence of external forces, \vec{n} will assume in a continuous manner all possible orientations throughout the bulk fluid. Such a macroscopically unaligned nematic might be viewed as a poly(liquid)crystalline sample, with the direction of \vec{n} arbitrarily determined by boundary conditions and defects (disclinations) within the fluid. Macroscopically aligned single (liquid) crystal samples may be prepared by orienting the nematic director via suitable container surface treatments or more conveniently for magnetic resonance experiments, by exploit-

ing the diamagnetic anisotropy characteristic of the nematic structure: $\Delta\chi = (\chi_{\parallel} - \chi_{\perp})$ where χ_{\parallel} and χ_{\perp} are the values of magnetic susceptibility parallel and perpendicular to \vec{n} , respectively. In moderate fields (> 0.1 Tesla), a nematic with $\Delta\chi > 0$ will rapidly orient (< 1 s) with the nematic director aligned parallel to the magnetic field; a uniaxial single (liquid) crystal is established with its optic axis along the field. For $\Delta\chi < 0$, \vec{n} is aligned normal to the field yielding a uniplanar distribution of the local nematic directors, i.e. a two-dimensional powder-like distribution of \vec{n} is established and the sample is characterized by susceptibilities χ_{\perp} in the field direction and $(\chi_{\parallel} + \chi_{\perp})/2$ at right angles to the field.

Molecular dynamics in nematics

Many of the molecular dynamical features of liquid crystals are very similar to those of ordinary liquids. The time scales for intra- and extra-molecular motions (isomerization or transitions among Rotational Isomeric States (RIS) and rigid-body motion) are arbitrarily differentiated and categorized in Table 1A. The key differences between isotropic liquids and liquid crystals are subtle and involve both extra-molecular rotation and translation. Rotational diffusion of prolate molecules is inherently anisotropic even in isotropic liquids but this anisotropy appears to be exaggerated in the liquid crystal: rotational diffusion about the minor semi-axes of the prolate mesogen is encumbered in the nematic fluid. There is also evidence for anisotropy in the translational diffusion; diffusion along the director being enhanced relative to that normal to \vec{n} by a factor of two. There is an additional dynamical mode unique to liquid crystals: fluctuation of the director about its equilibrium orientation⁷. There have been intensive efforts to probe the molecular dynamics of low molecular mass liquid crystals and contrast them with ordinary liquids using n.m.r. relaxation in order to ascertain exactly how director fluctuations, in addition to the more conventional dynamical processes, modulate nuclear spin interactions. It is, however, the combination of liquid-like dynamics and spatial anisotropy that makes liquid crystals uniquely suited to n.m.r. investigations: nuclear hyperfine interactions (dipolar and quadrupolar) that are averaged to zero in isotropic liquids are accessible in liquid crystals via essentially high resolution n.m.r. techniques⁸. Hence, both molecular structural features of mesogens and molecular organiza-

Table 1 Schematic breakdown of dynamical processes

A Dynamical processes in a nematic	Rate $1/\tau$ (s^{-1})
1. RIS transitions	$10^{10} - 10^{12}$
2. Rigid-body tumbling (anisotropic)	$10^7 - 10^{10}$
3. Self-diffusion; $\tau \approx (\chi^2)/2D$ (anisotropic; for $\chi = 10 \text{ \AA}$)	$10^7 - 10^8$
4. Director fluctuations (collective elastic modes)	$10^5 - 10^9$
B Dynamical processes in a polymer fluid	Rate $1/\tau$ (s^{-1})
1. RIS transitions	$10^{10} - 10^{12}$
2. Segmental reorientation (anisotropic libration)	$10^7 - 10^{10}$
3. Self-diffusion along chain contour; $\tau \approx (\chi^2)/2D$ (reorientation of \vec{r}_e via reptation; for $\chi = 100 \text{ \AA}$)	$10^2 - 10^7$
4. Fluctuations of principal strain direction (collective elastic modes)	'overdamped'

tional features of liquid crystal phases can be investigated with n.m.r.

Entangled polymer fluids

As in liquid crystals there are unique organizational and dynamical aspects of the long chain molecules in entangled polymer fluids. Hence, we try to construct an analogous hierarchy of structural and dynamical features of polymer fluids. The equilibrium properties of flexible, linear chains composed of covalently linked monomer units can most conveniently be described with idealized models of a polymer such as the freely jointed chain or random flight chains having successive bond directions uncorrelated⁹. These model chains follow Gaussian statistics in the limit of an infinitely long chain. In real chains, however, the inherent flexibility of the linkages between monomers is insufficient to satisfy the requirement of negligibly small orientational correlations between successive monomer units. This difficulty is reasonably avoided by rescaling the polymer chain to yield an equivalent chain of hypothetical segments each comprised of several actual monomer units. Such a hypothetical or Kuhn segment k is illustrated schematically in *Figure 1*. The equivalent polymer chain of hypothetical segments can in turn be partitioned into subchains which span the distance r_e between *entanglements* (permanent covalent crosslinks and/or transient topological constraints)¹⁰. In fluid phases (neat melts or concentrated solutions) of chains having dimensions that exceed the *entanglement molecular weight*, the lateral excursions of a given subchain are encumbered by its complement of neighbouring chains, i.e. the subchain is confined by a penetrable *tube* with a diameter on the order of tens of Angstroms^{2,11}. Coarsely we can identify the *tube* with its associated locally uniaxial constraint as a superficial analogue to the *nematic cage* in the liquid crystalline fluid. In a quiescent polymer fluid or relaxed elastomeric network the *tube* axes would assume random orientations; in a sheared fluid or a deformed elastomer network, a non-random distribution would be applicable. A uniaxial (nematic-like) distribution would be obtained if elongational flow or simple tension were applied to a polymer fluid and an elastomeric network, respectively.

Dynamics of entangled chains

The dynamical attributes of a condensed polymer fluid are indicated in *Table 1B*. The principal motions can be coarsely subdivided into two processes: intrachain dynamics and whole chain transport properties. The former are driven by rapid isomerization about primary bonds in the real chain, a process that leads to variably restricted reorientation of the equivalent chain's hypothetical segments. This is similar to the anisotropic molecular motion in liquid crystals. Isotropic reorientation of the chain segments is only affected by the slower, translational diffusion of the chain along its contour length through the maze of neighbouring chains, i.e. diffusion through a randomly oriented sequence of connected tubular confinements in the entangled polymer fluid (*reptation*)^{2,11}. The rate of this latter process, equivalently described in terms of its influence on the n.m.r. properties as the reorientation of *tube* axes r_e , is inversely proportional to the square of the chain's mass. We conclude this brief comparison of liquid crystals and polymer fluids by speculating that in macroscopically aligned uniaxial polymer fluids and elastomeric networks, the motional

analogue to director fluctuations is probably overdamped.

DEUTERIUM NUCLEAR MAGNETIC RESONANCE

Dynamical and structural information about deuterium labelled molecules in oriented, fluid phases is particularly accessible with D n.m.r. The labelling of the molecule is innocuous: specific hydrogens are exchanged for deuterons without altering the dimensions of the molecule. In the ordered phase, the anisotropic motion of the labelled molecule manifests itself in the D n.m.r. spectra in the form of resolved quadrupolar doublets, $\Delta\nu$, one for each of the orientationally (motionally) inequivalent sites in the molecule. The magnitude of $\Delta\nu$ is directly related to the average orientation of the C–D bond vector relative to the symmetry axis (director) of the oriented phase. (For the uniaxial phases depicted in *Figure 1*, each of the $\Delta\nu$ is further attenuated by the factor $P_2(\cos\Omega) = \frac{1}{2}(3\cos^2\Omega - 1)$, where Ω is the angle between \mathbf{n} and \mathbf{B} .) The usefulness of D.n.m.r. becomes evident when it is possible to decompose the average orientation of the C–D bond vectors into two contributions: (1) averaging caused by the anisotropic rigid-body reorientation of each conformer of the labelled molecule; (2) averaging due to intramolecular motion—reorientations of the C–D bond vector generated by transitions among the possible conformers. The former contribution would scale all of the $\Delta\nu$ in a multiply labelled flexible molecule whereas the latter contribution would be reflected in the relative differences in the magnitudes of the $\Delta\nu$. In principle, therefore, it is possible to extract internal structural information from flexible molecules using D n.m.r.⁴

Although the primary subject of this article is limited to studies of oriented, fluid phases, it should be emphasized that D n.m.r. is a very valuable technique for investigating structure and dynamics in *isotropic* liquids and solids. In liquids, D n.m.r. lineshapes and relaxation times are dominated by the quadrupolar interaction and dynamical information may be obtained in the conventional ways¹². In immobilized glasses and solids, the D n.m.r. lineshapes exhibit a very explicit dependence on the detailed manner in which the C–D bond vector exercises restricted reorientations. In the past few years this feature of the use of D n.m.r. to monitor macromolecular dynamics has advanced considerably; Spiess has succinctly reviewed such applications of D n.m.r. to solid polymers¹³.

Herein we will focus on recent D n.m.r. investigations from our laboratory involving oriented fluid phases including uniaxially deformed polymer phases, chain-like solutes dissolved in nematic solvents, and linear thermotropic polymer liquid crystals. We will review these systems drawing analogies with the organization and dynamics in low molar mass liquid crystals.

The quadrupolar interaction

The D n.m.r. spectra of deuterium labelled solids and anisotropic fluid phases are dominated by the interaction of the deuteron nuclear quadrupole moment with the residual electric field gradient (*efg*) at the nucleus¹⁴. Defining the applied magnetic field \mathbf{B} to lie along the z -axis, the first order perturbation of the Zeeman levels is given by

$$E_m = [eQV_{zz}/4hI(2I-1)][(3m^2 - I(I+1))] \quad (1)$$

E_m is expressed in frequency units and for the deuteron $I=1$; eQ is the quadrupole moment and V_{zz} is the z component of the efg tensor. V_{zz} is in turn related to a locally defined efg tensor at the deuteron. For aliphatic deuterons, we define such a local tensor in a principal cartesian X,Y,Z -frame with the Z -axis along the C-D bond vector; the principal value is denoted $V_{zz}=eq$, and the asymmetry parameter $\eta=(V_{xx}-V_{yy})/V_{zz}$ with the convention $|V_{yy}|\leq|V_{xx}|\leq|V_{zz}|$, i.e.

$$V = eq \begin{pmatrix} -\frac{1}{2}(1-\eta) & 0 & 0 \\ 0 & -\frac{1}{2}(1+\eta) & 0 \\ 0 & 0 & 1 \end{pmatrix} \quad (2)$$

and

$$V_{zz} = eq \left[(3\cos^2\theta - 1)/2 + \frac{\eta}{2}\sin^2\theta\cos 2\phi \right]$$

where θ and ϕ are, respectively, the polar and azimuthal angles locating \mathbf{B} in the X,Y,Z -frame. (eQV/h is called the quadrupole coupling tensor, e^2qQ/h is the quadrupole coupling constant, and $3e^2qQ/4h = \nu_Q$ is referred to as the quadrupole interaction constant.) The aliphatic quadrupole coupling constant $eQV_{zz}/h = e^2qQ/h = 168$ kHz and $\eta = 0.04^{15}$.

The quadrupolar perturbation of the Zeeman levels results in two transitions centered about the chemically shifted frequency $\nu_0 = (1 - \sigma_{zz})B/2\pi$. The separation between the two transitions (the quadrupolar splitting) is given by

$$\Delta\nu = 3eQV_{zz}/2h \quad (3)$$

Orientalional distributions

For a static distribution of C-D bond vectors relative to \mathbf{B} , the D n.m.r. spectrum or lineshape $I(\nu)$ is a superposition of quadrupolar splittings. The intensity of $I(\nu)$ is weighted by the orientational distribution function $W(\theta, \phi)$:

$$I(\nu) = \int_0^\pi \int_0^{2\pi} \frac{1/T_2}{[(\nu - (\nu_0 - \Delta\nu/2))^2 + (1/T_2)^2]} W(\theta, \phi) d\theta d\phi \quad (4)$$

where we have assumed the transitions to be Lorentzians of linewidth $1/T_2$.

The appearance of the static or *rigid limit* spectra are illustrated in the top traces in Figure 2. Two cases are shown: (1) a static, isotropic distribution of the C-D bond vectors (referred to as a Pake powder spectrum) having $W(\theta, \phi)d\theta d\phi = \sin\theta d\theta d\phi$; (2) a uniplanar distribution of the C-D bond vectors (a 2-D powder spectrum) having the plane tangent to \mathbf{B} , i.e. $W(\theta, \phi)d\theta d\phi = W(\pi/2, \phi)d\phi$.

Molecular motion

The character of the *rigid limit* spectrum is substantially modified if the C-D bond vectors are allowed to reorient at a sufficiently rapid rate. The quantity determining the limiting rate $1/\tau$ (in s^{-1}) is the *average* quadrupolar interaction constant $\bar{\nu}_Q$. For a solid this is the *rigid limit* value $\Delta = 3eQV_{zz}/4h$ ($\sim 1.25 \times 10^5 s^{-1}$ for aliphatic deuterons). For *slow* ($1/\tau < \Delta$) and *intermediate* ($1/\tau \approx \Delta$) reorientational rates, $I(\nu)$ is particularly sensitive to the type of reorientation mechanism (libration, jumps, rotational diffusion, etc.). This sensitivity has been exploited

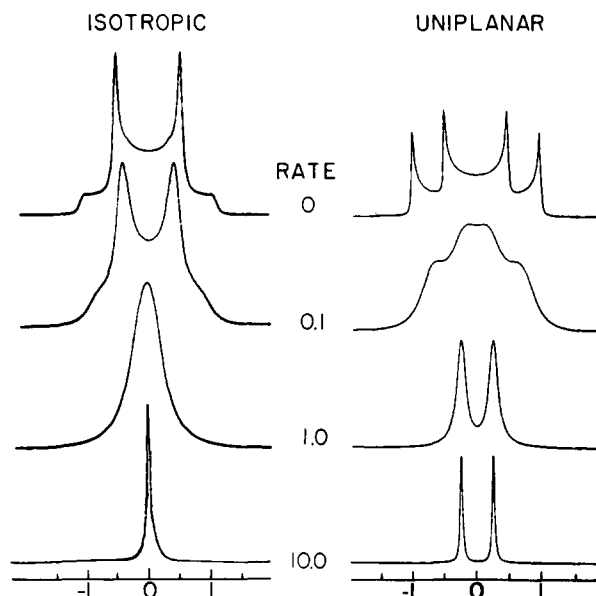


Figure 2 Simulated n.m.r. spectra for isotropic (left) and uniplanar (right) distributions of C-D bond vectors as a function of the rate of reorientation of the vectors; the rate $1/\tau$ is in units of the average quadrupolar interaction constant $3eQV_{zz}/4h$ which was taken as unity and the linewidth $1/T_2 = 0.013$ (in the same units). The reorientational jumps are random but preserve the initial C-D bond vector distributions; for the uniplanar distributions, the plane is tangent to \mathbf{B}

to obtain the reorientational rate $1/\tau$ (and the amplitude) of specific types of motion^{13,16}.

In Figure 2 the effect of C-D bond vector reorientation is illustrated with the evolution of $I(\nu)$ for increasing jump-rates (random jumps in θ - ϕ space) subject to the initial distributions, *isotropic* powder and 2-D *uniplanar* distribution, respectively. With increasing jump rate the *rigid limit* spectra transform into the *ultra-fast exchange limit* spectra (bottom traces in Figure 2). For the isotropic case, very rapid random reorientation of the C-D bond vector ($1/\tau \geq 10\Delta \approx 10^7 s^{-1}$), the motion averages the efg tensor to zero ($V_{zz} = 0$) and the spectrum collapses to a sharp Lorentzian singlet with a linewidth independent of $1/\tau$. By contrast, the uniplanar distribution together with the rapid motion leaves a residual, averaged efg tensor. Correspondingly, a resolved quadrupolar doublet persists with a splitting determined by the motionally averaged efg tensor. If we assume the local efg tensor is uniaxial ($\eta = 0$) and the C-D bond (Z -axis) is constrained to reorient in the plane, the rapid motion averages the relevant component of the efg tensor to $V_{zz} = (V_{zz} + V_{xx})/2 = 1/4eq$ for the plane tangent to \mathbf{B} . The resulting $\Delta\nu = 3e^2qQ/8h$ is a factor of 4 smaller than the *rigid limit* maximum splitting with the C-D bond parallel to \mathbf{B} .

Ordered fluids

In the last idealized case showing the effects of rapid but anisotropic (uniplanar) motion, the observed $I(\nu)$ is suggestive of the kind of D n.m.r. spectrum we might anticipate from labelled molecules in liquid crystals and oriented fluid polymer phases. For uniaxial nematic-like fluids, it is convenient to specify the average orientation of the labelled molecule relative to the director \mathbf{n} with the Saupe order tensor s^{19} , a second rank, traceless tensor with elements:

$$S_{ij} = \langle (3I_i I_j - \delta_{ij})/2 \rangle \quad (5)$$

The brackets $\langle \dots \rangle$ indicate a time average taken over the rapid molecular motion; l_j are the direction cosines between \mathbf{n} and the j -axis of a cartesian frame fixed on the molecule (e.g. the X, Y, Z -frame with the Z -axis along the $C-D$ bond). The relevant component of the efg tensor (that along the magnetic field \mathbf{B}), averaged over the anisotropic rigid-body motion of the labelled molecule, is readily expressed by

$$V_{zz} = \frac{2}{3} \text{Tr}(\mathbf{V} \cdot \mathbf{S}) P_2(\cos \Omega) \quad (6)$$

where $\cos \Omega = \mathbf{n} \cdot \mathbf{B}$ and \mathbf{V} and \mathbf{S} are specified in a common molecular fixed frame.

For flexible molecules it is necessary to consider the additional motional processes that can average the efg tensor. We employ an equilibrium statistical mechanical average over all of the possible conformations, $\{\phi\}$, of a flexible molecule in the rotational isomeric state (RIS) limit⁹. The combination of the contributions from rigid-body reorientation and intramolecular reorientation to the observed quadrupolar splittings is formally expressed as^{20,21}

$$\Delta\nu = eQ/h \left[\sum_{\{\phi\}} P\{\phi\} \text{Tr}(\mathbf{V}\{\phi\} \cdot \mathbf{S}\{\phi\}) \right] P_2(\cos \Omega) \quad (7)$$

$P\{\phi\}$ is the probability of having conformation $\{\phi\}$ in the ordered fluid and depends on the internal energy of the conformation as well as energetic considerations associated with accommodating the conformation in the anisotropic environment. Both \mathbf{V} and \mathbf{S} may be functions of $\{\phi\}$. This functionality will be dependent on the frame in which these tensors are defined; clearly \mathbf{V} will be independent of $\{\phi\}$ if the local X, Y, Z -frame is employed.

In the absence of detailed descriptions of the molecular dynamics involved in averaging \mathbf{V} , and especially for cases with less than uniaxial symmetry (e.g. liquid crystals with monoclinic or orthorhombic symmetry), it is convenient to express the quadrupolar splittings in terms of the motionally averaged principal element of \mathbf{V} and the resulting asymmetry parameter, $e\bar{q}$ and $\bar{\eta}$, respectively:

$$\Delta\nu = \frac{3}{2} (eQ/h) \bar{e}\bar{q} [P_2(\cos \theta) + (\bar{\eta}/2) \sin^2 \theta \cos 2\phi] \quad (8)$$

θ and ϕ are the polar coordinates of \mathbf{B} in the local frame defining a homogeneous (orientationally uniform) domain in the liquid crystal. The parameters $e\bar{q}$ and $\bar{\eta}$ can be extracted by fitting the experimentally observed lineshape $I(\nu)$. It should be emphasized that while the local $\eta = 0$ for aliphatic deuterons, the motionally averaged asymmetry parameter $\bar{\eta}$ may differ substantially from zero; it will reflect the symmetry characteristics of the motion averaging the efg tensor²².

RESULTS AND DISCUSSION

Isotropic fluid polymers

In dilute solutions of deuterium labelled polymers composed of monomers that may isomerize about one or more bonds, the efg tensor is very effectively averaged to zero by rapid intra- and extra-molecular motion. Essentially high resolution D n.m.r. spectra (line widths ≤ 5 Hz) are observed for such isolated macromolecular independent of the polymer chain's length. In entangled fluid

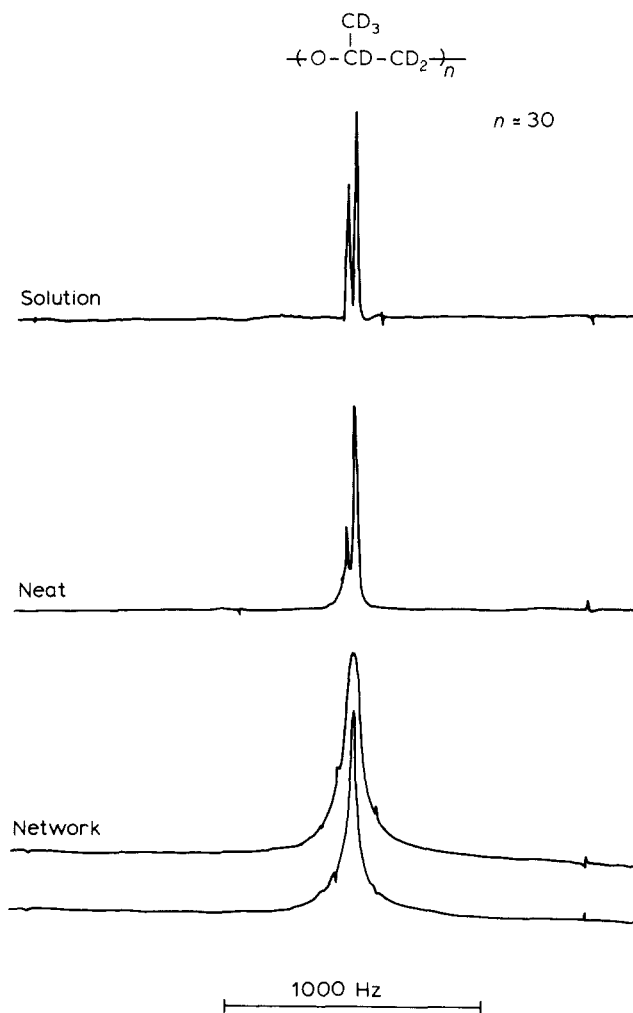


Figure 3 D n.m.r. spectra of poly(propylene oxide- d_6) at 13.8 MHz (non-spinning) $T = 300$ K. Top trace $\sim 1\%$ (wt) in chloroform solution; the neat polymer is methoxy terminated; the network was obtained by reacting the PPO- d_6 diol with a tricarboxylic acid chloride (see ref. 23). The bottom trace was obtained by spinning the network at ~ 100 Hz about an axis normal to \mathbf{B}

polymer phases, the spectra will be sensitive to the intrinsic chain flexibility and the dynamics of the larger scale chain reorientational processes. Figure 3 shows the kind of D n.m.r. spectra that the rather flexible elastomer poly(propylene oxide- d_6) (PPO- d_6) exhibits in dilute solution and in the neat fluid polymer phase. Even though this chain is rather short (degree of polymerization ≈ 30), on going from isolated chains (dilute solution) to the neat fluid phase there is some evidence of broadening of the resonance corresponding to the deuterons directly bonded to the main chain. Further restriction of the chain mobility by anchoring the chain ends (covalently reacting them) to form a 3-D network results in incompletely averaged quadrupolar interactions and a substantially broadened D n.m.r. spectrum (linewidth ~ 100 Hz). The identification of the broadening with the residual quadrupolar interactions can be verified; the linewidth is reduced by rapid spinning (~ 100 Hz) about an axis at right angles to the field (bottom trace Figure 3)²⁴.

Although PPO and poly(*cis*-isoprene) (PIP) have similar glass transition temperatures (205 K and 200 K, respectively), the double bond present in the latter reduces

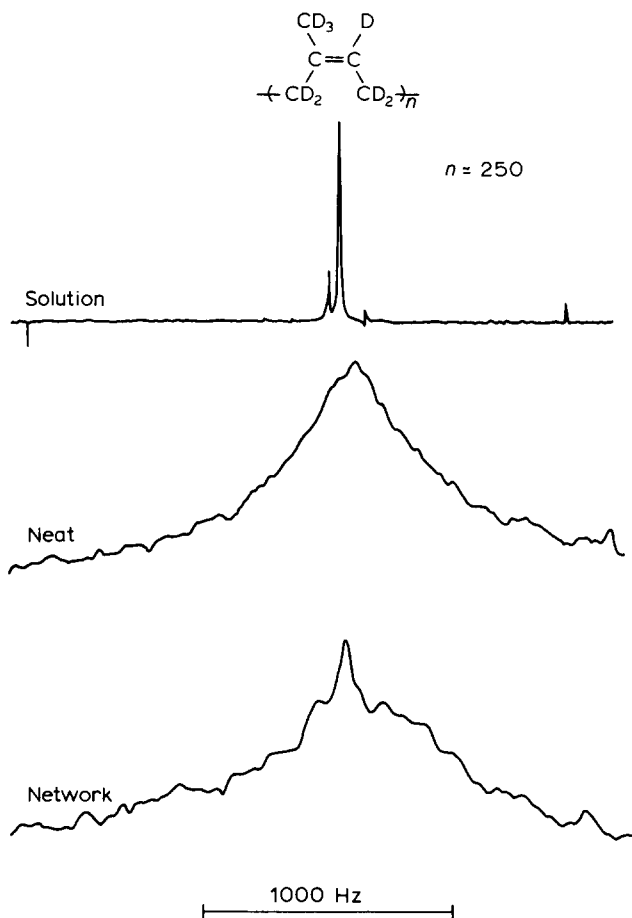


Figure 4 D n.m.r. spectra of *cis*-poly(isoprene- d_8) with the same conditions as *Figure 3*. The labelled network was synthesized by an end-linking reaction of diols with a triisocyanate (see ref. 25)

its intrinsic flexibility in the melt above T_g . This increased rigidity of the chain is not apparent in the dilute solution D n.m.r. spectrum of poly(*cis*-isoprene- d_8) (top trace *Figure 4*); in fact, it is possible to distinguish the chemically shifted methine deuteron from the aliphatic resonances in this essentially high resolution D n.m.r. spectrum. However, there is a dramatic increase in the line-width (to ~ 1 kHz) on removal of the solvent, i.e. the D n.m.r. spectrum of this neat fluid elastomer is dominated by the incompletely averaged quadrupolar interactions. Moreover, because of the comparatively large chain length and accompanying transient entanglements in this fluid, the relevant chain reorientational motions are not substantially changed on anchoring the chain ends; there is less than a factor of two increase in the D n.m.r. linewidth on forming the poly(isoprene) network (*Figure 4*).

The D n.m.r. spectra of the isotropic networks in *Figures 3* and *4* may be considerably broadened relative to high resolution spectra, but the residual quadrupolar interaction is very small relative to the *rigid limit* spectra. As shown in *Figure 5*, below T_g , both polymers exhibit *rigid limit* spectra spanning a ~ 250 kHz range (the linewidth of the superposed methyl component of each of these *rigid limit* spectra is reduced by a factor of 1/3 because of rapid rotation about the C_3 -axis). Hence, at 300 K, the residual quadrupolar interactions only amount to $\sim 1\%$ of the static values, i.e. the room

temperature spectra of the elastomer networks are near the *ultra-fast exchange limit* (*Figure 2*). Near this limit, the effective linewidth of the apparent Lorentzian resonance $1/T_2'$ is a very strong function of the temperature (*Figure 6*). In this regime an effective correlation time τ' characteristic of additional larger scale dynamical processes that may average the residual quadrupolar interactions can be introduced. The influence of such motions on the linewidth is given by¹⁴

$$1/T_2' = 1/T_2 + \frac{1}{5} \langle 3e^2qQ/2h \rangle^2 \tau' \quad (9)$$

where $\langle 3e^2qQ/2h \rangle$ is the residual quadrupolar splitting,

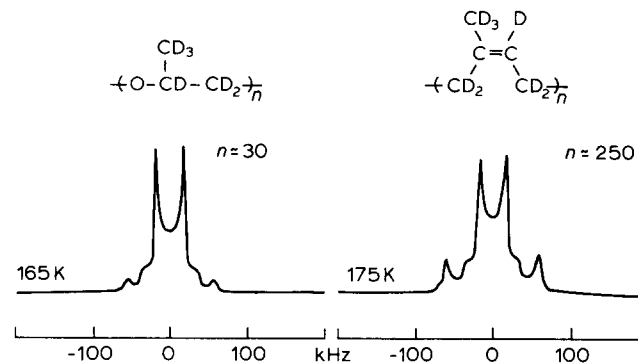


Figure 5 D n.m.r. spectra of PPO- d_8 and PIP- d_8 below their respective glass transitions at 46 MHz. The observed edge singularities correspond to the C-D (and CD_3 C_3 -axis) oriented normal to B . The methyl quadrupolar splitting is reduced by a factor of 1/3 relative to those of the C-D bonds on the mainchain

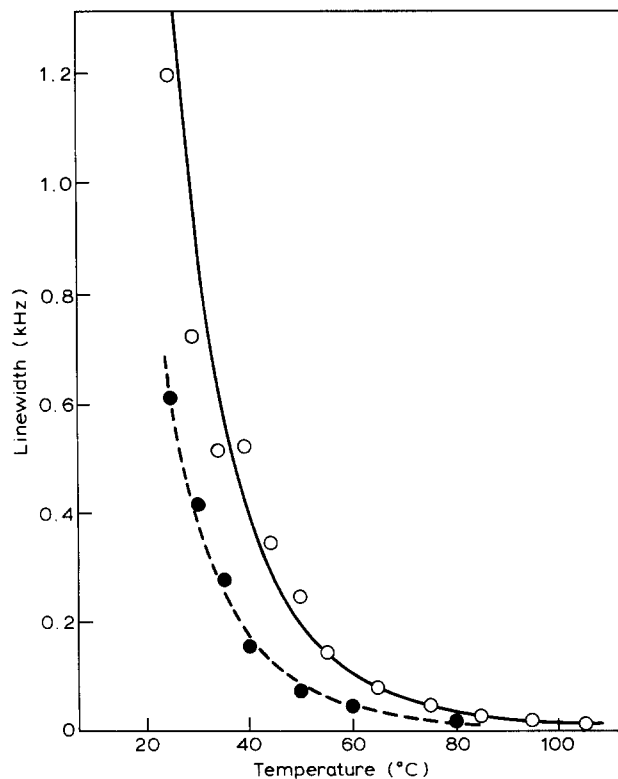


Figure 6 Apparent D n.m.r. linewidth ($1/T_2' - 1/T_2$) for PIP- d_8 polymer (●) and network (○) as a function of the temperature

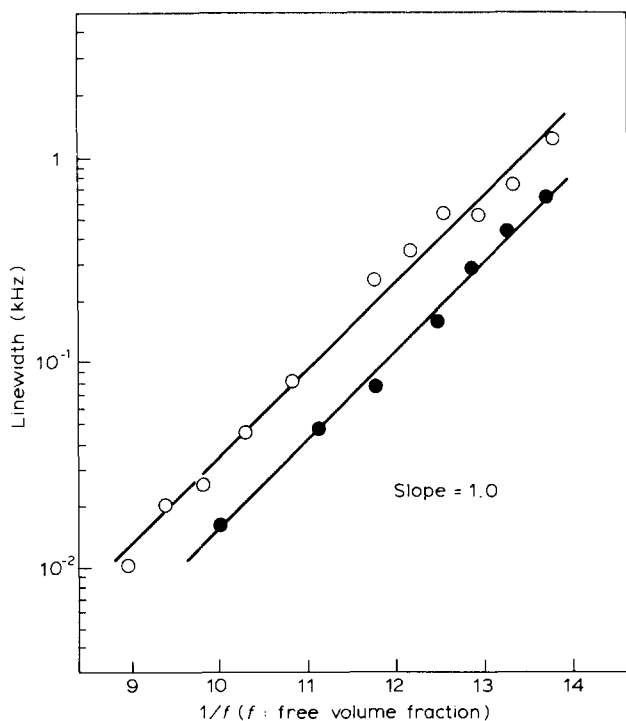


Figure 7 A semi-log plot of the apparent linewidth (data in Figure 6) versus the fractional free volume for the PIP- d_8 polymer (●) and network (○). The free volume fraction f at each temperature was calculated using: $T_g = 200\text{K}$, $f_g = 0.026$, $\alpha_f = 4.8 \times 10^{-4} \text{K}^{-1}$, $1/T_2 = 5 \text{Hz}$

i.e. the result of averaging the efg tensor over the rapid local motions.

Generally, these larger scale dynamical processes are activated when sufficient free volume is accessible in condensed polymer phases. The effective correlation time has been related to the average free volume fraction at a particular temperature, f , via $\tau' = A \exp(f^{-1})$, where A is a constant characteristic of the polymer²⁶. Williams, Landel and Ferry (WLF)²⁷ have expressed f by the linear function

$$f = f_g + a_f(T - T_g) \quad (10)$$

where f_g is the fractional free volume at the glass transition temperature and a_f is the thermal expansion coefficient of the free volume. With these definitions, in Figure 7 we demonstrate that such an analysis of the D n.m.r. linewidth data seems appropriate; the plot of $\ln(1/T^{*2} - 1/T_2)$ versus $1/f$ (a WLF plot) is linear.

Chain order via guest probe molecules

Uniaxially deformed polymers have structural similarities with nematic liquid crystals and consequently many of the techniques developed to study low molar mass liquid crystals may be applied to the polymer phases. In particular, these materials may be probed by studying the D n.m.r. spectra of a small amount of deuterium labelled guest molecule solubilized in the bulk phases.

Deformed elastomer networks. Deloche and myself demonstrated the feasibility of the probe approach with swollen networks under simple tension²⁸. The reorientation of the guest as it diffuses through the polymer host matrix reflects the anisotropy of the array of partially ordered chains; resolved quadrupolar splittings that scale

with the strain function ($\lambda^2 - \lambda^{-1}$) are exhibited by the guest probe. Typical D n.m.r. data from a uniaxially strained poly(*cis*-isoprene) network swollen to various degrees with benzene- d_6 is shown in Figure 8; $\lambda = L/L_0$ is the ratio of the deformed sample length to the original length.

In similar experiments on swollen networks subjected to uniaxial compression ($\lambda < 1$), the compression axis may be conveniently rotated relative to the field B . Figure 9 shows the angular dependence of the D n.m.r. spectra of benzene- d_6 ($\sim 5\%$) dissolved in a compressed poly(*cis*-isoprene) network. The morphology of the compressed sample may be anticipated to consist of a uniplanar distribution of radially oriented domains of extended chains; the local tube axes are on average aligned normal to the compression axis c . Hence, when $c \parallel B$ ($\Omega = 0^\circ$), a discrete quadrupolar doublet is observed with $\Delta\nu = 0.85 \text{kHz}$; when $\Omega = 55^\circ$, $P_2(\cos\Omega) = 0$ and the splitting disappears. At $\Omega = 90^\circ$, $I(\nu)$ is determined by the guest molecule's self-diffusion coefficient D : if the benzene diffusion is fast in the compression plane (if $\langle s^2 \rangle / 2D$ large relative to the inverse of the quadrupolar splitting, where s is an rms diffusion distance in the plane that corresponds to a ~ 1 -radian angular change in the orientation of a local domain symmetry axis), the guest probe can sample all domain orientations and a resolved doublet is observed with half the magnitude of that in the $\Omega = 0^\circ$ spectrum. If the diffusion is slow and only a few domains are samples, an incompletely averaged spectrum is exhibited.

Such findings exactly parallel guest molecule D n.m.r. studies of cholesteric liquid crystals, a phase with a uniplanar-like arrangement of uniaxial domains^{17,18}. In

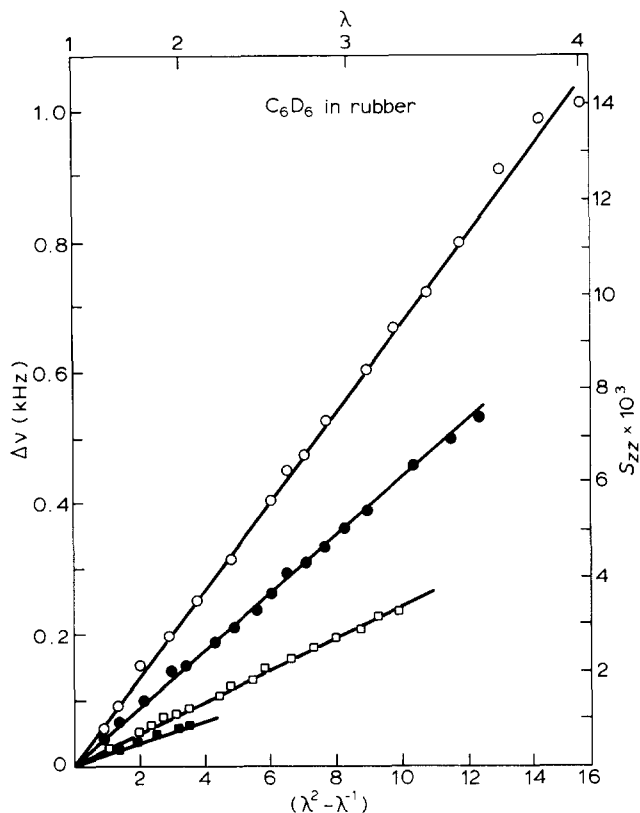


Figure 8 D n.m.r. quadrupolar splittings of benzene- d_6 at various concentrations in a uniaxially deformed crosslinked poly(isoprene) rubber; ϕ is the polymer volume fraction (○) $\sim \phi = 0.93$; (●) $\sim \phi = 0.80$; (□) $\sim \phi = 0.52$; (■) $\sim \phi = 0.32$: $\lambda = L/L_0$ is the deformation. $S_{zz} = \langle P_2(\cos\theta) \rangle$ is the order parameter of the benzene symmetry axis relative to n in the experiment is normal to B

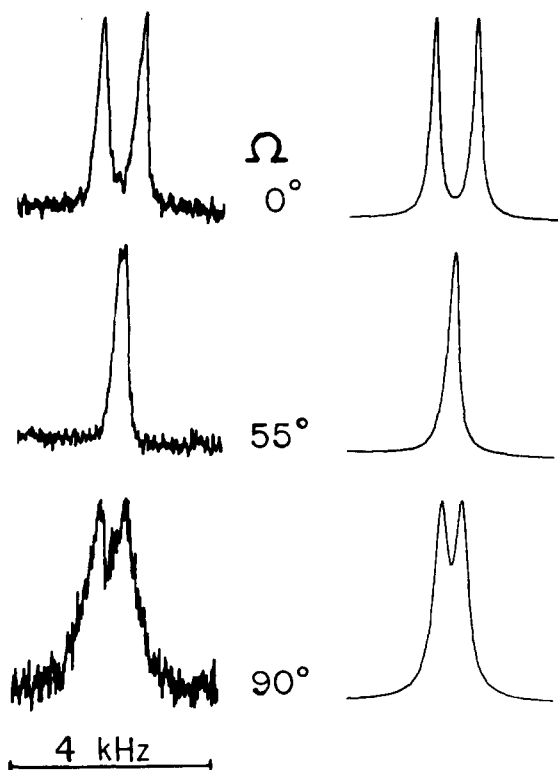


Figure 9 D n.m.r. spectra (left) of benzene- d_6 (2.5%wt) in a uniaxially compressed sample ($\lambda \approx 0.75$) of a crosslinked poly(isoprene) rubber as a function of the angle Ω between the compression axis c and B . Calculated lineshapes $I(\gamma)$ (right) are for an axial quadrupolar interaction undergoing planar reorientational diffusion with Ω the angle between the magnetic field and the normal to the plane. The diffusion rate $1/\tau = 0.9(1.7 \text{ KHz})$, where 1.7 KHz is the average quadrupolar splitting ($2\Delta\gamma[\Omega=0]$) and $1/T_2 = 200 \text{ Hz}$ (see ref. 18)

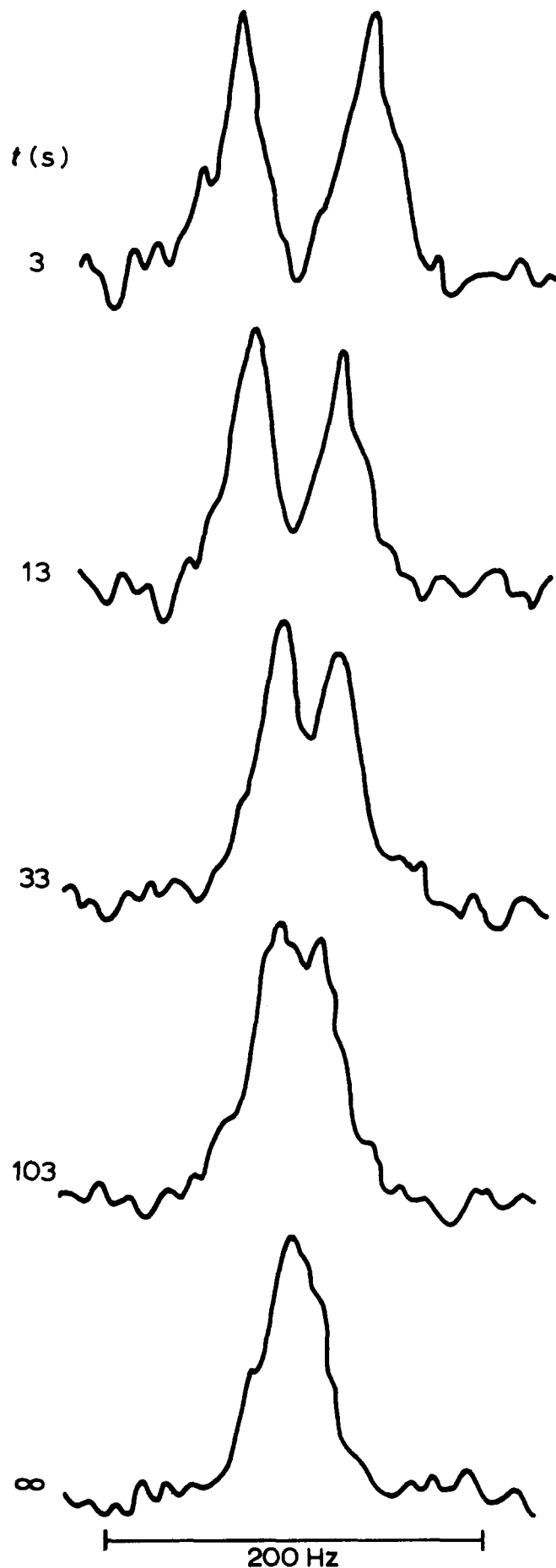


Figure 10 D n.m.r. spectra of benzene- d_6 ($\sim 0.5 \text{ wt\%}$) solubilized in a neat poly(isobutylene) fluid as a function of time after cessation of a simple shear deformation; 300 K

phases wherein the orientation of the local director n is *not* spatially invariant, diffusion of the guest probe molecule is tantamount to reorientation of n . The effect of increasing the rate of reorientation of n (increasing the guest diffusion rate) on the D n.m.r. spectra can be calculated in the same way illustrated in *Figure 2*. In *Figure 9* we contrast the angular dependence of the D n.m.r. spectra of benzene- d_6 in the compressed poly(isoprene) network with spectra calculated to account for similar data derived from cholesteric liquid crystals. The director reorientation rate used to simulate the spectra together with an independent measurement of the benzene self-diffusion coefficient (e.g. see ref. 29) would enable one to estimate the gradient of average chain orientation in the plane of compression.

Sheared elastomer fluids. It is possible to probe transient orientational phenomena in polymer fluids with D n.m.r. A sheared melt of high molecular weight poly(isobutylene) containing ($\sim 5\%$) benzene- d_6 will exhibit transient quadrupolar splittings after being subjected to an elongational shear strain. *Figure 10* shows the evolution of the benzene molecule's average orientation (in terms of its quadrupolar splitting) as a function of the time after cessation of the shear. Analysis of the data suggests at least two relaxation processes characterized by half-lives on the order of seconds and tens of seconds, respectively³⁰. As chain *equilibration* (accommodation of the average chain conformation to changes in the magnitude and orien-

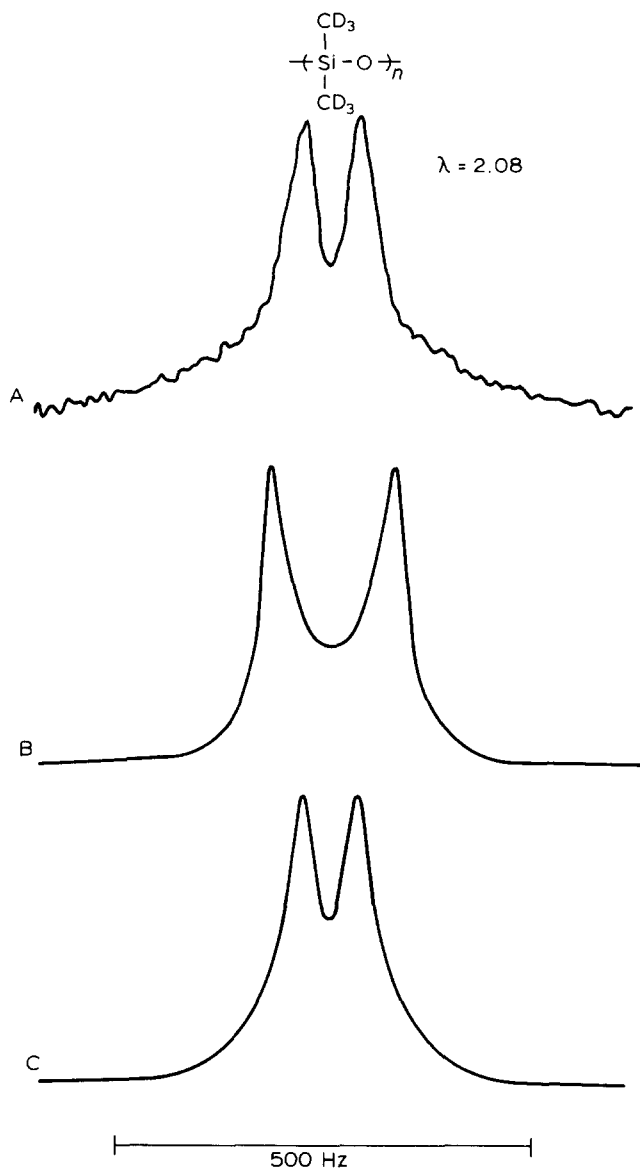


Figure 11 D n.m.r. spectra of poly(dimethyl siloxane- d_6) networks under a uniaxial tensile deformation with the principal strain director normal to \mathbf{B} . (A) Experimental spectrum (number average degree of polymerization $m=350$; ref. 34). (B) Simulated lineshape $I(\nu)$ with affine deformation of ideal network of identical chains. (C) as in (B) but with distribution of chain lengths (most probable distribution with a number average degree of polymerization = 350)

tation of r_e) is rapid^{31,32}, the transient orientational order observed with D n.m.r. reflects the slower processes. Conceivably retraction of the chain in the deformed tube as well as the slower reorientation of the tubes to their equilibrium isotropic distribution as the stress relaxes in the fluid could be investigated with D n.m.r. The time scales associated with the various relaxation processes that are operative after subjecting an entangled fluid to a step strain have been recently discussed³³.

D n.m.r. of labelled polymer chains

Deloche and coworkers have demonstrated that network chain segmental orientational order can be directly probed with D n.m.r. by studying a perdeuterated poly(dimethylsiloxane- d_6) network³⁴. At room temperature, the relaxed network shows a single resonance with a linewidth of ~ 25 Hz suggesting that the intramolecular motion of this inherently flexible polymer above T_g

very effectively averages the efg tensor even in the crosslinked network. Under simple tension, the network exhibits a partially resolved quadrupolar splitting that is proportional to $(\lambda^2 - \lambda^{-1})$. Figure 11A shows such a spectrum for a deformation ratio $\lambda = 2.08$.

Figure 11B and C show computed $I(\nu)$ based on affinely deformed networks composed of Gaussian chains. Using equation (8) with $\bar{\eta} = 0$, we have for the average of the efg tensor over the internal dimethylsiloxane segmental motion:

$$e\bar{q} = eqP_2(\cos 70.5^\circ)P_2(\cos 90^\circ)S_k \quad (11)$$

where the two Legendre polynomial factors account for the rapid reorientation of the C-D bond vector about the methy C_3 -axis and the orientation of the C_3 -axis at right angles to the segment symmetry axis, k . (We naively assume one dimethylsiloxane monomer corresponds to a single Gaussian chain segment.) $S_k = \langle P_2(\cos\theta_k) \rangle$ is the average orientation of a segment relative to the chain's end-to-end vector. In the Gaussian limit $S_k = 3\lambda^2/5n$, where n is the number of segments in the chain (degree of polymerization). The spectrum $I(\nu)$ is computed with equation (4) using an elliptical distribution for the orientation of the end-to-end vectors relative to the strain axis (affine deformation):

$$W(\theta, \phi) d\theta d\phi = \lambda^2 \sin\theta d\theta d\phi / (\cos^2\theta + \lambda^2 \sin^2\theta)^{3/2};$$

the isotropic limiting form for $W(\theta, \phi)$ is recovered in the undeformed network ($\lambda \rightarrow 1$).

In Figure 11B we assume an ideal network of identical chains having degree of polymerization $n = 350$; in Figure 11C, $I(\nu)$ is calculated by convoluting $W(\theta, \phi)$ with a most probable molecular weight distribution parameterized such that the average degree of polymerization $n = 350$. Gronski and coworkers advocate the importance of including the effect of chain length distributions and non-affine considerations to fit the observed $I(\nu)$ in recent D n.m.r. studies of uniaxially deformed, labelled poly(butadiene) networks³⁵.

In more refined calculations of $I(\nu)$ for labelled networks, we examine the assumption of $\bar{\eta} = 0$, the influence of rapid fluctuations of junctions (rapid reorientation of the chain end-to-end vector), and the identification of the Kuhn segment with a single monomer unit³⁶. Experimental advances on this topic include monitoring the behaviour of junctions and chain segments independently by specific labelling³⁵, the effect of swelling on labelled networks³⁷ and the relationship between the quadrupolar splittings exhibited by the labelled chain segments and those obtained from deuterium labelled guest probes³⁸.

Chains solubilized in a nematic liquid crystal

Proton n.m.r. has been used extensively in conjunction with deuterium n.m.r. to investigate the molecular structural details of small solutes dissolved (~ 1 wt%) in a nematic solvent⁴. Both rigid and flexible solutes have been studied; geometrical as well as mechanistic data (on modes of internal isomerization) is obtained³⁹. Studies of deuterium labelled alkyl chains in this way yield data relevant to a variety of systems including chains appended to mesogens themselves as well as chains integral to biological structures such as membranes⁴⁰. In Figure 12 we show the D n.m.r. spectra of three perdeuterated n-alkanes solubilized in a nematic solvent (ZLI-1167;

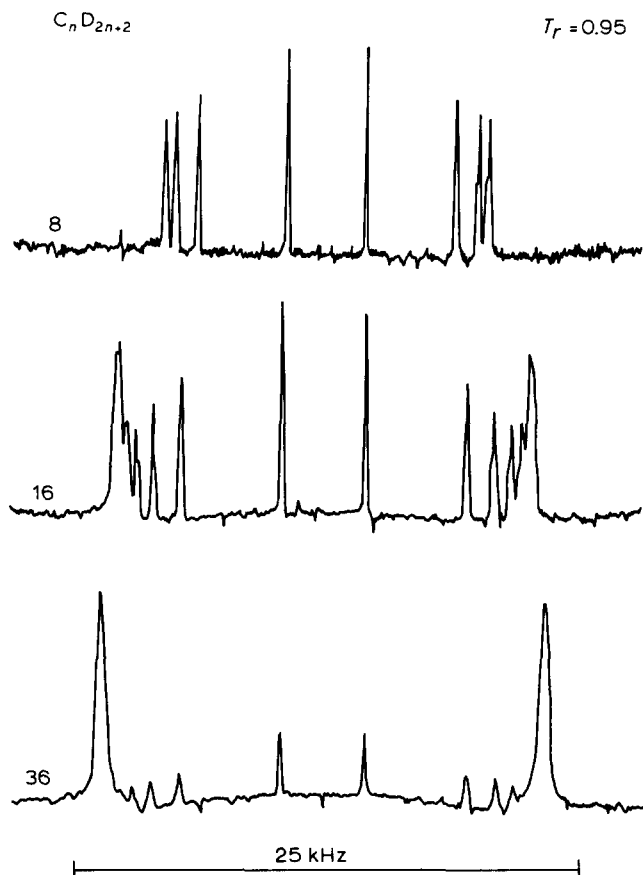


Figure 12 D n.m.r. spectra of perdeuterated n-alkanes (octane, hexadecane, hexatriacontane) solubilized ($\sim 1\%$ wt) in the nematic solvent ZLI1167 (Merck). The reduced temperature is relative to the apparent nematic-isotropic transition temperature in the respective solutions

Merck) at the same reduced temperature (i.e. the same degree of nematic order). Each of the labelled n-alkane homologues displays a discrete quadrupolar doublet $\Delta\nu_i$ for all of the i inequivalent CD_2 units and for the terminal CD_3 's. A sequential examination of the quadrupolar splitting patterns of n-alkanes enables an inductive assignment of $\Delta\nu_i$. The methyl doublet is the most intense and has the smallest splitting; the rotation about the C_3 -axis averages the efg by an additional factor of $P_2(\cos 70.5^\circ) = -1/3$. The next largest quadrupolar splitting is from the (equivalent) penultimate CD_2 segments, the next from the antepenultimate CD_2 segments, and so on; the central internal methylene segment(s) exhibit(s) the largest $\Delta\nu_i$. In short, for a given chain length, the $\Delta\nu_i$ asymptotically converge to the limiting values exhibited by the methylenes near the centre of the chain. With the exception of the first few CD_2 units near the chain termini, the internal CD_2 units are equivalent in terms of their propensity for averaging the efg tensor. Additionally, the spectra show a tendency for increased solute orientational order with increasing chain length, i.e. as the number of carbons in the alkane solute increases, the values of the internal CD_2 quadrupolar splittings increase. It appears that the rigid-body reorientational motion responsible for averaging all of the efg tensors is attenuated as the chain length increases.

In order to obtain the alkyl chain flexibility from the D.n.m.r. spectra (Figure 12), we have modelled the subtle variations in the observed quadrupolar splitting patterns. Such modelling enables a determination of the extent to

which the flexible solute is perturbed in the uniaxial solvent, i.e. whether or not the chain flexibility is significantly different from that anticipated for a 'free' chain—an alkane in an isotropic environment. In order to investigate such relative differences in the chains, we have employed an equilibrium statistical mechanical average over alkane conformations sampling internal dihedral angles in the rotational isomeric state approximation. For our purposes, we have found a phenomenological model of an isolated chain constrained by its environment to be sufficient.

The inertial frame (IF) model that we used to calculate quadrupolar splittings exhibited by labelled flexible molecules has been described before^{21,40}. Originally developed to explain the D n.m.r. spectrum exhibited by n-octane- d_{18} dissolved in a nematic solvent⁴¹, it has been applied to labelled alkyl chains appended to nematic²⁰ and discotic⁴² liquid crystals. Qualitatively, the IF model visualizes each alkane conformer as constrained by a cylindrical cavity which mimics the uniaxial mean field (assumed to be repulsive in nature) that the nematic solvent imposes on the alkane. The strength of the repulsive interaction is parameterized via the cavity radius. This repulsive energy is added to the usual RIS energies thereby perturbing the conformer's probability of occurrence ($P\{\phi\}$ in equation (7)) to favour those molecular shapes compatible with a uniaxial environment. In the nematic solvent, the alkane solute's conformer probabilities are given by

$$P\{\phi\} = Z^{-1} \exp(-U\{\phi\}/kT) \quad (12)$$

where $U\{\phi\}$ includes the additional energetic contribution attributed to the uniaxial constraint imposed on each conformer as well as the usual RIS energies; Z is the partition function.

The alkane quadrupolar splittings may be calculated with equation (7) using the IF model by specifying the alkane solute's orientational order tensor $S\{\phi\}$ —both its magnitude and the orientation of its principal axis frame for each conformer. The crux of the IF model is the identification of the principal frame of the order tensor as the frame that diagonalizes the inertia tensor of each conformer. This identification is consonant with a repulsive- or shape-dominated picture of solute ordering in the nematic mean field; prolate solute conformers on average align with their 'long molecular axis' parallel to the local nematic director.

As *trans* states are preferable to *gauche* states in alkanes, generally speaking, the nematic solvent favours the lower energy, more extended alkane conformers (conformers with a minimal number of *gauche* RIS). For example, an optimized fit of the IF model calculations to the observed quadrupolar splittings of octane in the nematic requires the probability of the *all-trans* conformer $P\{\phi = 0^\circ\} = 0.12^{21}$. This value is enhanced by a factor of ~ 2 relative to that of the isolated 'free' chain ($P\{\phi = 0^\circ\} = 0.05$). Such implied conformational perturbations for the flexible chain in the nematic solvent are, moreover, very sensitive to the primary structure of the solute chains. In diglyme (the analogue to n-nonane with carbons, 2, 5 and 8 replaced with oxygens), the *gauche* RIS at C-C bonds 3 and 6 are energetically favoured, i.e. the low energy conformers are less extended than those of the analogue alkane⁹. Hence, when diglyme is solubilized in a

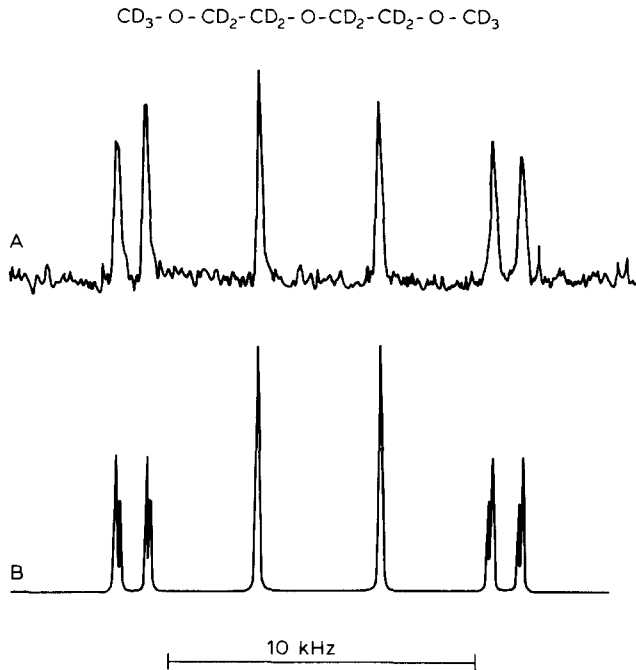


Figure 13 D n.m.r. spectra of diglymer- d_{14} solubilized ($\sim 1\%$) in the nematic solvent Phase 5 (Merck; $T_r = 0.98$). The largest splitting corresponds to the innermost methylenes in the chain and the smallest to the terminal methyl groups. In the simulated spectrum (B) this assignment is confirmed using the IF model with a cavity radius similar to that employed for simulating the spectrum of *n*-decane- d_{22} (see ref. 21)

nematic the uniaxial mean field exerts significantly larger distortions of this molecule relative to those observed for an alkane. The D n.m.r. spectrum of diglyme- d_{14} can be described with the IF model (Figure 13) and the model implies that the diglyme chain's $P\{\phi = 0^\circ\}$ increases by a factor of 6 (relative to the 'free' chain value $P\{\phi = 0^\circ\} = 0.02$) when it is constrained in the nematic solvent⁴³.

The implied enhancement of the RIS energetics associated with dissolving (distorting) the oxyethylene chain in a nematic appears to be substantiated by the n.m.r. spectra of similarly solubilized poly(ethylene- d_4 glycols). Figure 14 shows that with increasing degree of polymerization, the magnitude of the CD_2 quadrupole splittings decrease. (Contrast this with the observations of the *n*-alkanes (Figure 12).) This is presumably indicative of a trade-off, with increasing chain length, between the RIS internal energy (favouring more globular conformers of the oxyethylene chain with the lower energy *gauche* RIS populated) and the influence of the nematic uniaxial constraint (favouring extended conformers).

Polymeric liquid crystals

Over the last twenty-five years a variety of solutions and melts of certain semi-flexible polymers have been shown to exhibit lyotropic and thermotropic phases. Perhaps the most thoroughly studied polymeric liquid crystals are the cholesteric phases formed in solutions of the rod-like, helical synthetic polypeptides⁴⁴. Poly(γ -benzyl-L-glutamate) (PBLG), Figure 15a, in particular has been shown to exhibit all of the characteristics of low molar mass liquid crystals. In the mid-1960's, it was discovered independently in three different laboratories that in moderate magnetic (and electric) fields, the cholesteric structure in PBLG solutions could be untwisted to

yield an aligned nematic phase suitable for carrying out n.m.r. studies⁴⁵. In fact, PBLG appears to have been the first oriented polymer in which quadrupolar interactions were investigated with D.n.m.r.⁴⁶ There was, however, an extant effort to study hydration in fibrous proteins (collagen) and DNA using the residual quadrupolar interactions in D_2O ⁴⁷.

In the magnetically aligned PBLG liquid crystals, quadrupolar splittings of both labelled solvents and labelled polypeptides can be readily observed^{48,49}. Figure 15b shows the D.n.m.r. spectra of PBLG- d_7 ; in the liquid crystal the helices are aligned parallel to the director n (and B). The restricted motion of the labelled sidechains is reflected in the magnitude of the quadrupolar splittings. It is noteworthy to mention that the two deuterons in the benzyl methylene group are not equivalent (labelled A and B in Figure 15b), and that this difference changes with temperature and solvent reflecting changes in the average orientation of the labelled sidechain on the periphery of the PBLG helix⁵⁰.

In isotropic solid samples of PBLG- d_7 , powder spectra indicative of intrasidechain mobility are observed at room temperature (e.g. Figure 15c shows evidence for rapid reorientation about the ring para-axis plus libration of this axis). Moreover, as magnetically oriented (*single crystal*) solid PBLG films can be prepared by evaporating the solvent from the liquid crystalline solutions in the presence of a magnetic field⁴⁵, both the angular de-

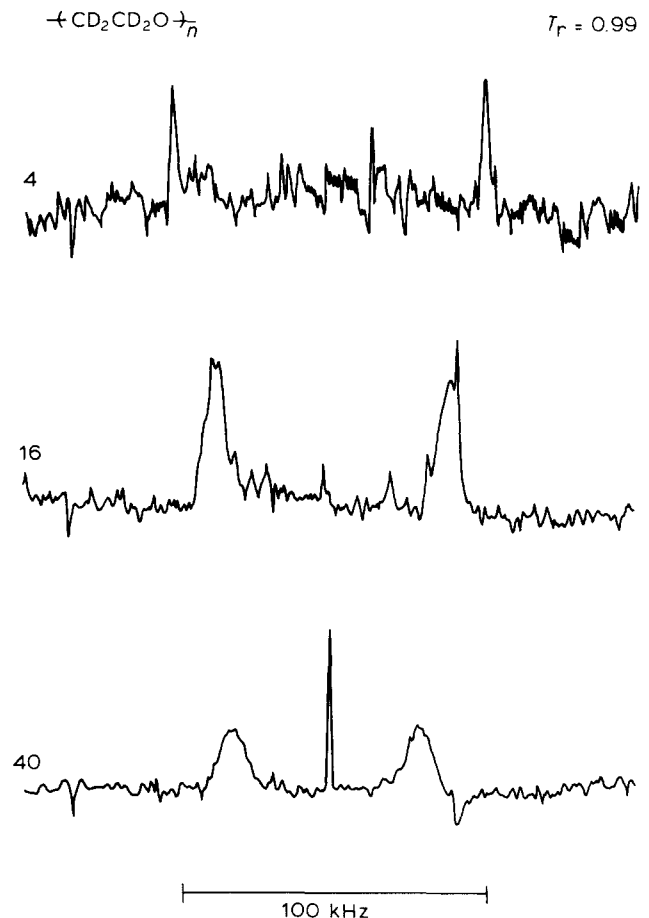


Figure 14 D n.m.r. spectra of poly(ethylene glycol- d_4) solubilized ($\sim 2\%$ wt) in the nematic solvent Phase 5 (Merck) as a function of the degree of polymerization of the chain; in the bottom trace some phase-separated isotropic solution contributes the central resonance

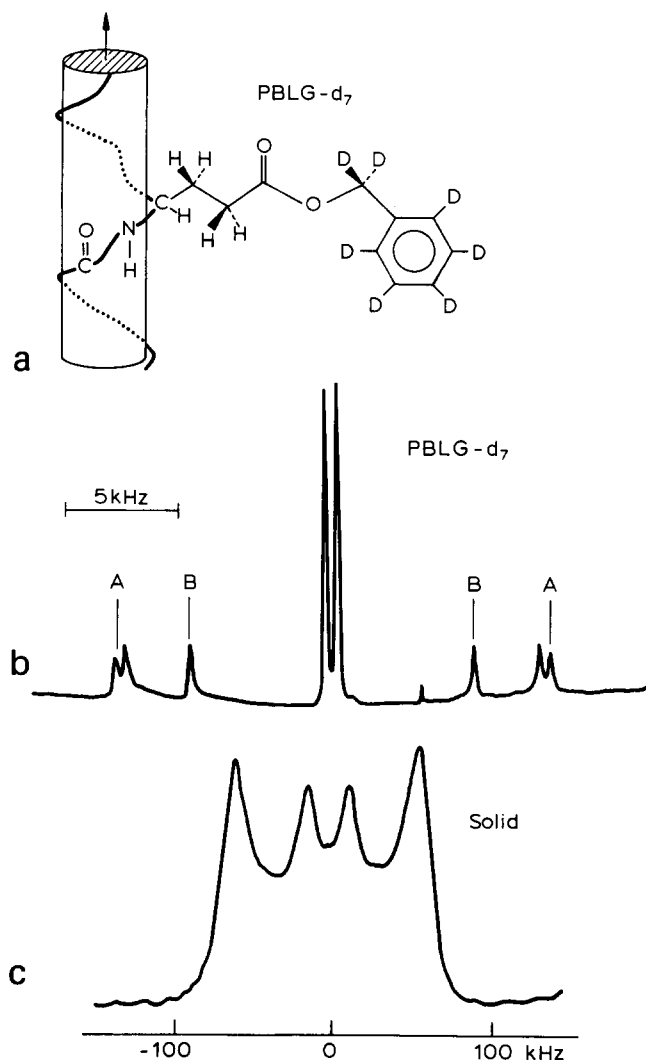


Figure 15 (a) Structure of poly($-\gamma$ -benzyl-L-glutamate- d_7) (PBLG- d_7) sidechain appended to an α -helix. (b) D n.m.r. spectrum of a PBLG- d_7 liquid crystal (30% polymer in dioxane), 300 K; the resonances of the benzyl methylene deuterons are indicated A and B. (c) Solid state D n.m.r. spectrum of PBLG- d_7 (isotropic powder), 300 K, 46 MHz

pendence and the temperature dependence of the D.n.m.r. lineshapes in oriented, *solid* PBLG- d_7 films can be exploited to give unique structural insights into the mobility and packing of the sidechains in the solid state of this polypeptide⁵¹.

Thermotropic polymeric liquid crystals may be readily synthesized by judiciously combining prolate mesogenic cores and flexible chains. Comb-like polymers with the mesogenic sidechains connected to the main chain by a labelled, flexible, alkyl *spacer* have been studied with D n.m.r.; the extent of dynamic coupling of the mesogenic sidechains to the main chain (mobility of the spacer) has been investigated⁵².

An alkyl chain experiences maximum extension in a fluid phase when it is embedded in the main chain of a linear polymer liquid crystal—a polymer composed of rigid, mesogen cores alternating with a flexible *alkyl spacer*. In neat nematic melts of such polymers, the high orientational correlations between the mesogenic cores on both ends of the spacer impart additional constraints on the spacer chain's conformational freedom. These restrictions may be idealized by saying that the spacer chain's 'terminal bonds' (mesogenic cores) will strive to

stay mutually co-parallel in the nematic melt. For a highly stretched chain, this is only possible when there are an *odd* number of bonds in the spacer. For alkyl chains with an *even* number of bonds, the first and last 'bond' of the spacer tends to differ in orientation by roughly the carbon-carbon valence angle.

These posited differences between *even* and *odd* spacer lengths in linear polymeric liquid crystals should be reflected in the D n.m.r. spectra of suitably labelled polymers. Figure 16A shows such a spectrum of the nematic phase of a polymer with a labelled *even* spacer attached to the mesogenic cores by ester linkages⁵³. Basically two quadrupolar doublets are observed; the low intensity doublet with the maximum splitting was tentatively assigned to the α - CD_2 groups at both ends of the spacer. The eight internal methylenes were thought to have their splittings superposed (i.e. equivalent residual *efg* tensors). Extensions of the IF model to simulate D n.m.r. spectra of polymeric liquid crystals with labelled spacer chains (arbitrarily lengthening the terminal bonds of an analogue alkane) confirm this assignment (calculated spectrum, Figure 16B) and, moreover, suggest that the quadrupolar splitting pattern for a spacer having an *odd* number of methylenes should be qualitatively different from that with an *even* number (calculated spectrum for a nine-methylene spacer, Figure 16C). Confirmation of this last prediction remains to be demonstrated. Changes in the quadrupolar splitting patterns associated with the mode of linking the *spacer* to the mesogenic cores (ether linkages *versus* ester linkages) have been observed experimentally⁵⁴ and rationalized theoretically⁴³.

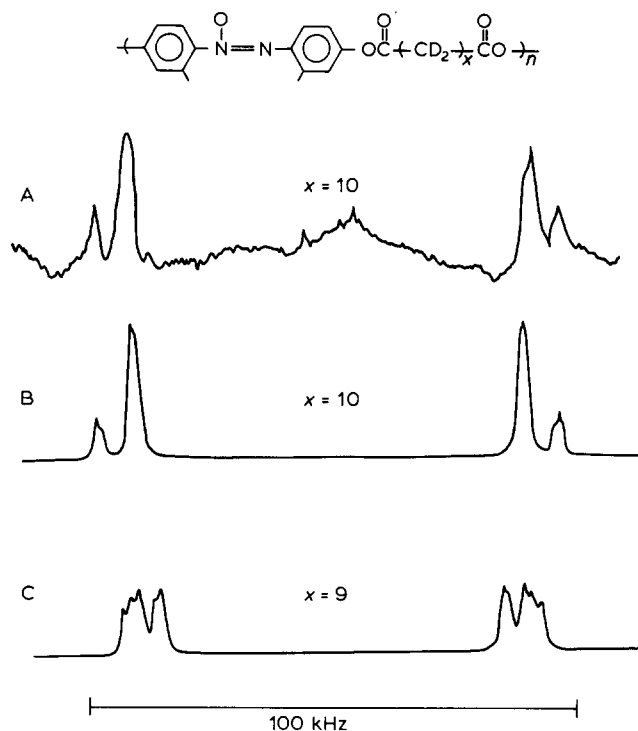


Figure 16 D n.m.r. spectra of a linear polymeric liquid crystal with a labelled alkyl chain spacer. (A) Experimental spectrum, 350 K. (B) Simulated spectrum using IF model, ten-carbon spacer. (C) Simulated spectrum of a nine-carbon spacer

CONCLUDING REMARKS

Residual quadrupolar interactions in the D n.m.r. spectra of labelled (and 'probed') fluid polymers, especially in phases exhibiting macroscopic order, give new and direct insights into the molecular dynamics and organization in this important state of matter. In networks and sheared fluids the larger scale attributes of chains are sampled; the orientation distribution (and its evolution in time) of the (sub)chain's end-to-end vector is accessible through D n.m.r. Also, explicit information about local chain properties can be studied with D n.m.r.; modelling quadrupolar splittings exhibited by labelled chains in nematic solvents is intimately linked to local dihedral angle preferences—to the magnitudes of the rotational isomeric state statistical weights. Such applications of D n.m.r. to labelled oligomers may provide a novel way to evaluate RIS parameters in the liquid state. The comparative perspective employed herein draws heavily on the use of the D n.m.r. in studies of low molar mass liquid crystals and suggests that the methodologies used so successfully there might be readily transferred to research on fluid phases of entangled polymers.

ACKNOWLEDGEMENTS

I am indebted to Bertrand DeLoche and Hirokazu Toriumi for many stimulating conversations during the course of our investigations, to J. S. Higgins and H. Yu for samples of labelled polymer chains, to L. Jelinski and E. Meirovitch for solid state spectra, and Z. Luz and R. Poupko for help with spectral simulations. The research was supported by the NSF (INT-8213 113) and the NIH (AM 17497).

REFERENCES

- 1 Bird, R. B. and Curtiss, C. F. *Physics Today* 1984, **37**, 36
- 2 de Gennes, P.-G. *Physics Today* 1983, **36**, 33
- 3 Samulski, E. T. *Physics Today* 1982, **35**, 40
- 4 See special issue on 'NMR in Liquid Crystals', *Israel J. Chem.* 1983, **22** (Ed. Z. Luz)
- 5 Kelker, H. and Hatz, R. 'Handbook of Liquid Crystals', Verlag Chemie, Weinheim, 1983
- 6 Gelbart, W. M. *J. Phys. Chem.* 1982, **86**, 4298
- 7 Warner, M. *Molec. Phys.* 1984, **52**, 677
- 8 Wade, C. G. *Ann. Rev. Phys. Chem.* 1977, **28**, 47; Emsley, J. W. and Lindon, J. C. 'NMR Spectroscopy using Liquid Crystal Solvents', Pergamon Press, Oxford, 1975
- 9 Flory, P. J. 'Statistical Mechanics of Chain Molecules', Wiley (Interscience), New York, 1969
- 10 Cohen-Addad, J. P. and Dupere, R. *Polymer* 1983, **24**, 400; Cohen-Addad, J. P. *Polymer* 1985, **26**, 197
- 11 Edwards, S. F. *Polymer* 1985, **26**, 163
- 12 Huntress, Jr., W. T. *Adv. Magn. Res.* 1970, **4**, 1, (Ed. J. S. Waugh), Academic, NY
- 13 Spiess, H. W. *Coll. Polym. Sci.* 1983, **261**, 193
- 14 Abragam, A. 'The Principles of Nuclear Magnetism', Oxford University Press, Oxford, 1961
- 15 Dong, R. Y. *Can. J. Phys.* 1978, **56**, 678
- 16 Schwartz, L. J., Meirovitch, E., Ripmeester, J. A. and Freed, J. H. *J. Phys. Chem.* 1983, **87**, 4453, and references cited therein
- 17 Samulski, E. T. and Luz, Z. *J. Chem. Phys.* 1980, **73**, 142
- 18 Luz, Z., Poupko, R. and Samulski, E. T. *J. Chem. Phys.* 1981, **74**, 5825
- 19 Saupe, A. *Z. Naturforsch.* 1965, **20a**, 572
- 20 Samulski, E. T. and Dong, R. Y. *J. Chem. Phys.* 1982, **77**, 5090
- 21 Samulski, E. T. and Toriumi, H. *J. Phys. Chem.* in press
- 22 Goldfarb, D., Poupko, R., Luz, Z. and Zimmermann, H. J. *Chem. Phys.* 1983, **79**, 4035
- 23 Higgins, J. S., Ma, K. and Hall, R. H. *J. Phys. C: Solid State Phys.* 1981, **14**, 4995
- 24 Cohen-Addad, J. P. and Roby, C. J. *J. Chem. Phys.* 1975, **63**, 3095
- 25 Hinkley, J. A. *PhD Thesis*, University of Wisconsin, 1978
- 26 Fujita, H., Kishimoto, A. and Matsumoto, K. *Trans. Faraday Soc.* 1960, **56**, 424; Fujita, H. and Kishimoto, A. *J. Chem. Phys.* 1961, **34**, 393
- 27 Williams, M., Landel, R. F. and Ferry, J. D. *J. Am. Chem. Soc.* 1955, **77**, 3701
- 28 Deloche, B. and Samulski, E. T. *Macromolecules* 1981, **14**, 575
- 29 von Meerwall, E. and Ferguson, R. D. *J. Polym. Sci. Polym. Phys. Edn.* 1981, **19**, 77
- 30 Samulski, E. T., unpublished results
- 31 Doi, M. and Edwards, S. F. *J. Chem. Soc. Faraday Trans.* 1978, **74**, 1789, 1802, 1818; 1978, **75**, 32
- 32 Doi, M. *J. Polym. Sci. Polym. Phys. Edn.* 1980, **18**, 1005, 2055
- 33 Viovy, J. L., Monnerie, L. and Tassin, J. F. *J. Polym. Sci. Polym. Phys. Edn.* 1983, **21**, 2427
- 34 Deloche, B., Beltzung, M. and Herz, J. *J. Phys. Lett. (Paris)* 1982, **43**, L-763
- 35 Gronski, N., Stadler, R. and Jacobi, N. M. *Macromolecules* 1984, **17**, 741
- 36 Nakatani, A. and Samulski, E. T., in preparation
- 37 Dubault, A. and Deloche, B., in preparation
- 38 Toriumi, H., Deloche, B. and Samulski, E. T., in preparation
- 39 See, for example, Poupko, R., Luz, Z. and Zimmermann, H. J. *Am. Chem. Soc.* 1982, **104**, 5307
- 40 Samulski, E. T. *Israel J. Chem.* 1983, **22**, 329
- 41 Samulski, E. T. *Ferroelectrics* 1980, **30**, 83
- 42 Samulski, E. T. and Toriumi, H. *J. Chem. Phys.* 1983, **79**, 5194
- 43 Yu, L. P. and Samulski, E. T. *Macromolecules* (submitted)
- 44 Samulski, E. T. 'Liquid Crystalline Order in Polymers', (Ed. A. Blumstein), Ch. 5, 167, Academic Press, New York, 1978
- 45 Sobajima, S. *J. Phys. Soc. Jpn.* 1967, **23**, 1070; Panar, N. and Phillips, W. D. *J. Am. Chem. Soc.* 1968, **90**, 3880; Samulski, E. T. and Tobolsky, A. V. *Macromolecules* 1968, **1**, 555
- 46 Chapman, G. E., Campbell, I. D. and McLauchlan, K. A. *Nature* 1970, **225**, 639
- 47 Berendsen, H. J. C. in 'Water. A Comprehensive Treatise', (Ed. F. Franks), Plenum, New York, **5**, 293 (1975)
- 48 Samulski, E. T. and Berendsen, H. J. *J. Chem. Phys.* 1972, **56**, 3920
- 49 Samulski, E. T. *J. Physique Coll., C3* 1979, **40**, C3-471
- 50 Czarniecka, K. and Samulski, E. T. *Mol. Cryst. Liq. Cryst.* 1981, **63**, 205
- 51 Meirovitch, E. and Samulski, E. T. (in preparation)
- 52 Geib, H., Hisgen, B., Pschorn, U., Ringsdorf, H. and Speiss, H. W. *J. Am. Chem. Soc.* 1982, **104**, 917; Boeffel, C., Hisgen, B., Pschorn, U., Ringsdorf, H. and Speiss, H. W. *Israel J. Chem.* 1983, **22**, 000
- 53 Samulski, E. T., Gauthier, M. W., Blumstein, R. and Blumstein, A. *Macromolecules* 1984, **17**, ???
- 54 Griffin, A. C. and Samulski, E. T. *J. Am. Chem. Soc.*, submitted